

Electronic Supplementary Information (ESI)

Visible light induced efficient hydrogen production through semiconductor-conductor-semiconductor (S-C-S) interface formed between g-C₃N₄ and rGO/Fe₂O₃ core-shell

Nithya Thangavel ^a, Sankeerthana Bellamkonda ^b, Abraham Daniel Arulraj ^a, G. RangaRao ^b, Bernaurdshaw Neppolian, ^{a,*}

^a SRM Research Institute and Department of Chemistry, SRM Institute of Science & Technology, Kattankulathur, Chennai - 603203, Tamil Nadu, India.

^b Department of Chemistry, Indian Institute of Technology Madras, Chennai - 600036, Tamil Nadu, India.

*E-mail: nepolian.b@res.srmuniv.ac.in

Content

1. **Figure S1.** XRD patterns of GO and rGO
2. **Figure S2.** Raman Spectra of GO and rGO
3. **Figure S3.** XPS survey scan spectra of g-C₃N₄/rGO/Fe₂O₃
4. **Figure S4.** Transient photocurrent measurement of g-C₃N₄, g-C₃N₄/rGO, g-C₃N₄/rGO/Fe₂O₃, rGO/Fe₂O₃
5. **Figure S5.** Mott-Schottky plot for (A) g-C₃N₄ (B) Fe₂O₃
6. **Figure S6.** Photocatalytic activity of optimization of rGO on g-C₃N₄
7. **Table 1.** Comparison of H₂ production efficiency of reported Pt loaded g-C₃N₄ based composites and without Pt loaded g-C₃N₄ composite catalysts (this work).

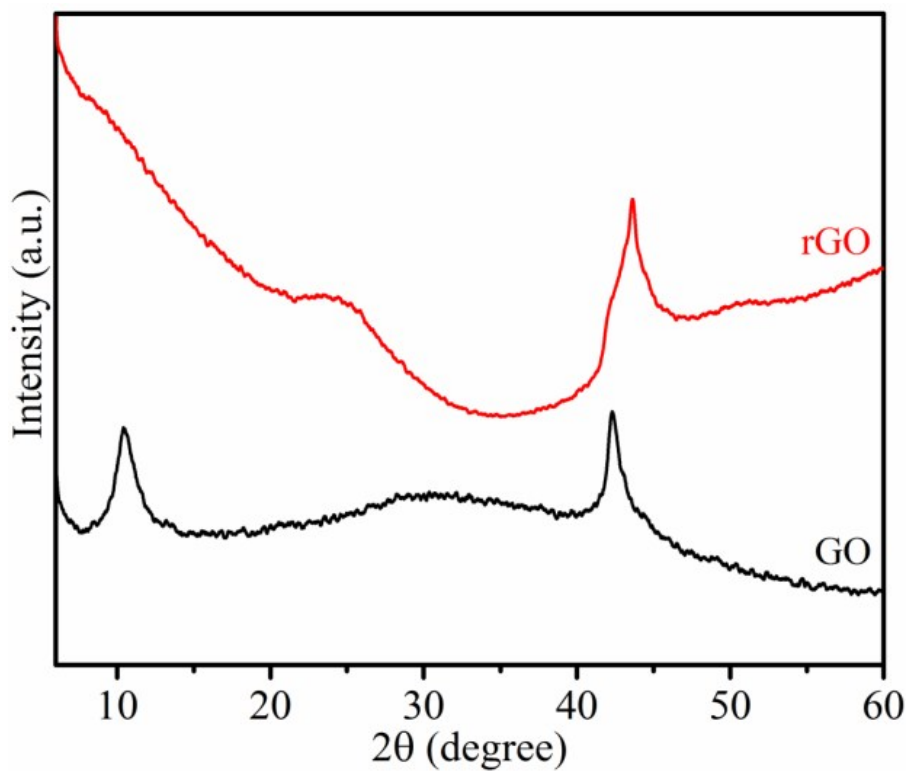


Figure S1. XRD patterns of GO and rGO

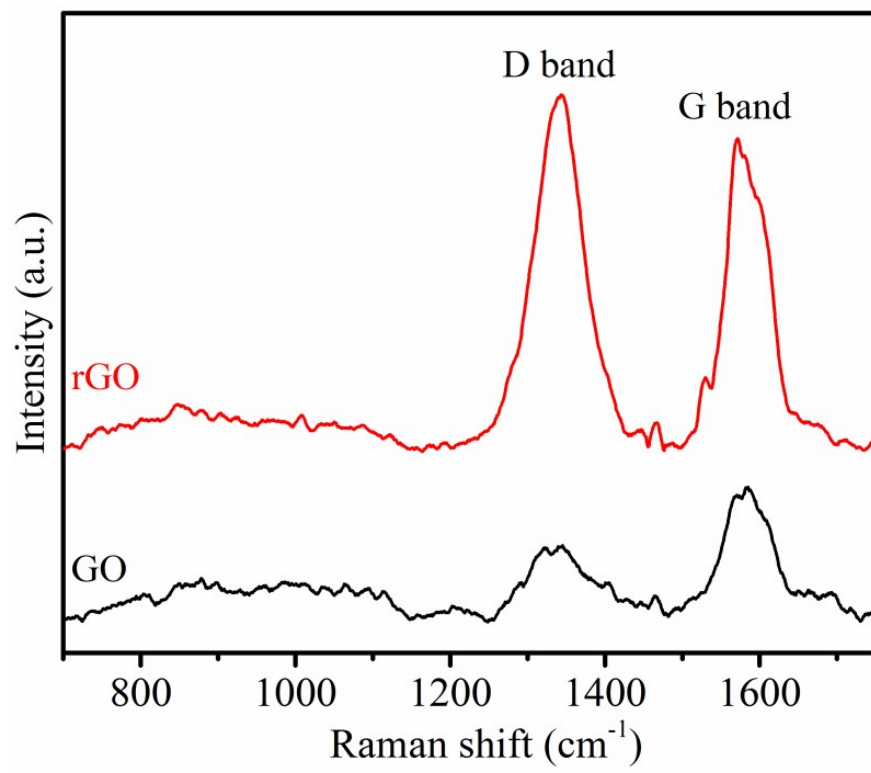


Figure S2. Raman Spectra of GO and rGO

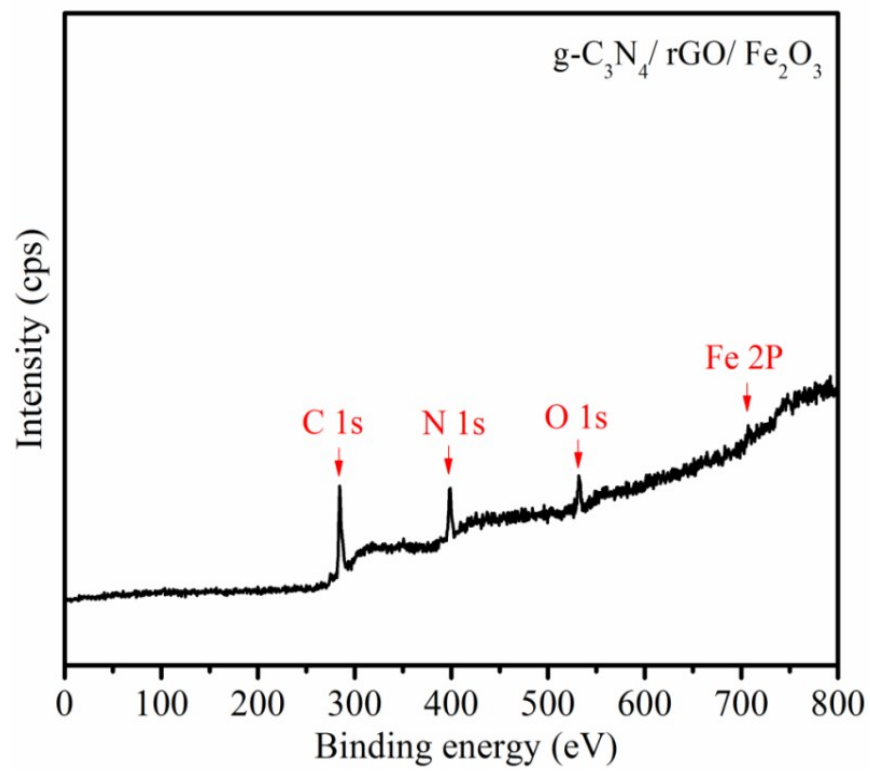


Figure S3. Photoemission survey scan spectra of $\text{g-C}_3\text{N}_4/\text{rGO}/\text{Fe}_2\text{O}_3$

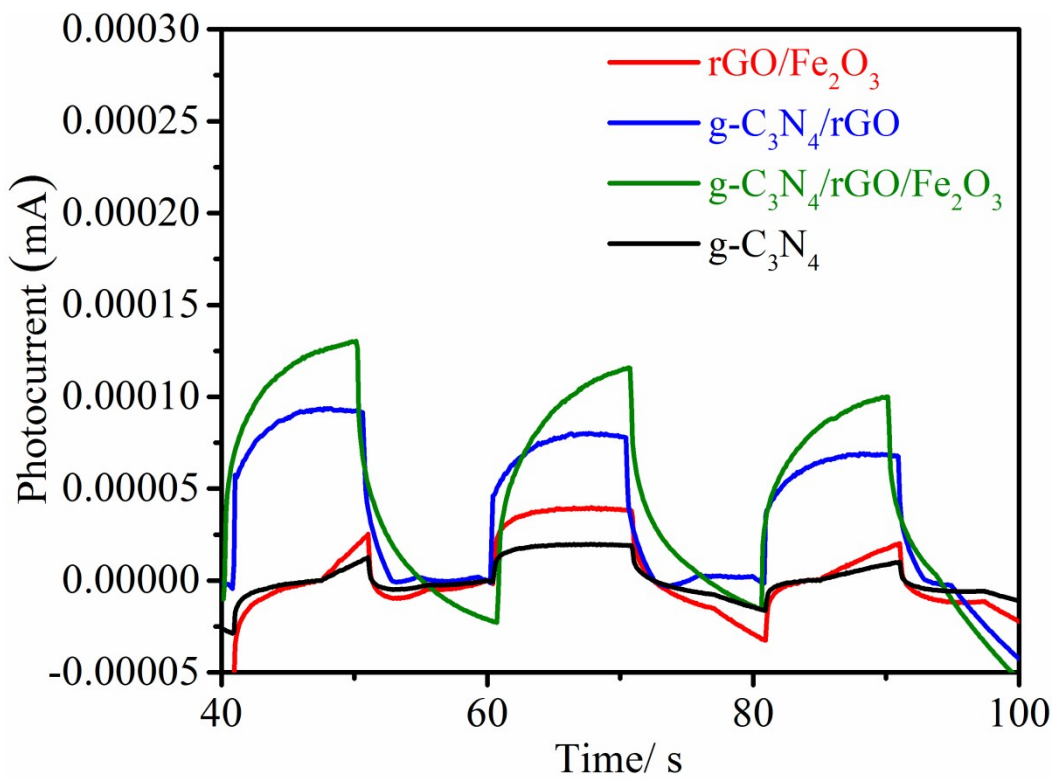


Figure S4. Transient photocurrent measurement of g-C₃N₄, g-C₃N₄/rGO, g-C₃N₄/rGO/Fe₂O₃, rGO/Fe₂O₃

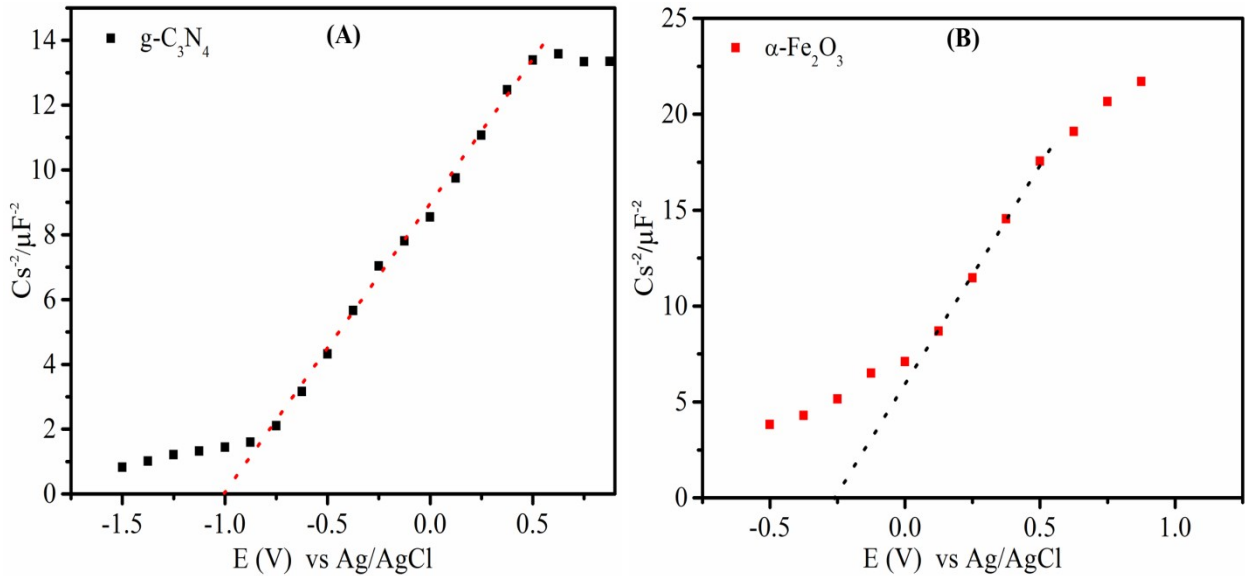


Figure S5. Mott-Schottky plot for (A) $\text{g-C}_3\text{N}_4$ (B) Fe_2O_3

The Mott-Schottky analysis was performed to calculate the flat band potential of $\text{g-C}_3\text{N}_4$ and Fe_2O_3 . As shown in Fig. S5, both $\text{g-C}_3\text{N}_4$ and Fe_2O_3 exhibits n-type characteristics curves. The flat band potential of $\text{g-C}_3\text{N}_4$ and Fe_2O_3 was found to be -1.0 V and -0.25 V vs Ag/AgCl at pH 7 (equivalent to -1.19 V and -0.44 vs. NHE at pH 7).

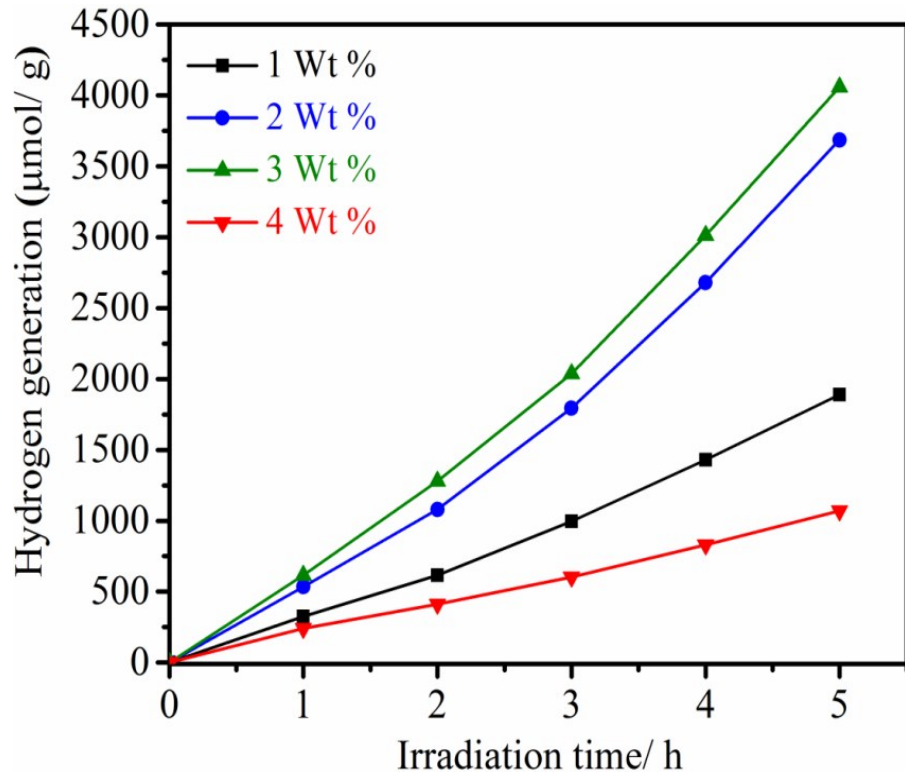


Figure S6. Photocatalytic activity of optimization of rGO on g-C₃N₄

Table S1 Comparison of H₂ production efficiency of reported Pt loaded g-C₃N₄ based composites and without Pt loaded g-C₃N₄ composite catalysts (this work).

Catalysts	Co-catalysts	Light Source	Sacrificial agents	H ₂ Evolution Rate (μmol g ⁻¹ h ⁻¹)	Quantum Yield (%)	Ref.
α-Fe ₂ O ₃ /2D-C ₃ N ₄	Pt	300 W Xe, λ > 400 nm	Triethanolamine (TEOA)	31400	44.35 (420 nm)	21
g-C ₃ N ₄ / zinc phthalocyanine	Pt	350 W Xe, λ ≥ 420 nm	Ascorbic acid	12500	1.85 (700 nm)	55
g-C ₃ N ₄ / PEDOT	Pt	300 W Xe, λ ≥ 420 nm	TEOA	327	NA	56
g-C ₃ N ₄ / WO ₃	Pt	300 W Xe, λ ≥ 420 nm	TEOA	110	0.9 (420 nm)	57
g-C ₃ N ₄ / N-GQDs	Pt	300 W Xe, λ ≥ 420 nm	TEOA	2180	5.25 (420 nm)	58
g-C ₃ N ₄ /TiO ₂	Pt	300 W Xe, λ ≥ 420 nm	TEOA	1780	NA	12
Nanospherical g-C ₃ N ₄	Pt	300 W Xe, λ ≥ 420 nm	TEOA	13675	9.6 (420 nm)	59
B-doped C ₃ N ₄ Nanosheets	Pt	300 W Xe, λ ≥ 420 nm	TEOA	5560	NA	60
Hollow C ₃ N ₄ Nanospheres	Pt	300 W Xe, λ > 420 nm	TEOA	4480	7.5 (420 nm)	61
C _x N-TiO ₂ /g-C ₃ N ₄	-	300 W Xe, λ > 420 nm	TEOA	39	NA	62
g-C₃N₄/ Fe₂O₃/rGO	-	250 W Xe,	TEOA	6607	NA	This work